

Stacking-fault model for the Si(111)-(7×7) surface

P. A. Bennett, L. C. Feldman, Y. Kuk, E. G. McRae, and J. E. Rowe

Bell Laboratories, Murray Hill, New Jersey 07974

(Received 2 March 1983; revised manuscript received 28 June 1983)

We propose a model for the geometric structure of the Si(111)-(7×7) surface based on a stacking fault in the surface layers. The model quantitatively accounts for existing ion-channeling data. Additional evidence for the stacking fault is given by constant-momentum-transfer averaged low-energy electron-diffraction data. A specific class of superlattice structures is suggested by the occurrence of two nearly equivalent stacking sequences having triangular symmetry.

The Si(111)-(7×7) surface is probably the most studied of the reconstructed surfaces of semiconductors. However, the structural results from ion channeling both on this surface^{1,2} and on the laser annealed "(1×1)" surface² remain to be reconciled with other surface models. Ion-channeling measurements of the surface peak (SP) for normal incidence yield a result expected for a nearly bulklike surface, while for non-normal incidence the SP is larger than the expected bulklike result by nearly two full monolayers. This has been interpreted as two full monolayers that are displaced at least 0.4 Å perpendicular to the surface but are displaced less than 0.15 Å parallel to the surface.^{1,2} Such a structure has a large change in bond length that is chemically unreasonable, and we propose a new stacking-fault model that quantitatively accounts for the ion scattering data. The proposed structure is chemically much more appealing since no change in bond length is required. We present additional evidence for this type of reconstruction based on constant-momentum-transfer averaged (CMTA) low-energy electron-diffraction intensity profiles of the integral order reflections. A specific model for the Si(111)-(7×7) superlattice is suggested by the occurrence of two nearly equivalent stacking sequences.

Various stacking models of Si are shown in Fig. 1, which illustrates a side view of atomic positions in the (110) plane and the relevant channeling directions. The atom layers are labeled to elucidate the stacking sequence which is cubic . . . *AaBbCcAaB* in the nonfaulted structure [Fig. 1(a)]. Figure 1(b) illustrates a fault between the first and second layers . . . *AaBbCcAa|C*, and Figs. 1(c) and 1(d) illustrate a fault between the third and fourth layers, i.e., . . . *AaBbCc|BbC* and . . . *AaBbCc|Bb|A*. These two latter models correspond to an intrinsic fault and a twin stacking fault, respectively.³ It is immediately clear that such models are qualitatively in agreement with the ion-channeling data. In the absence of thermal motion, incidence in the normal direction corresponds to scattering from three monolayers of atoms (not necessarily the top three) for all four stacking sequences, including the bulk structure. However, for incidence in the [001] or [111] channeling direction the faulted models yield one to three extra monolayers of atoms visible to the beam.

A quantitative comparison of the ion scattering data requires a calculation of the surface peak, including thermal vibrations. In Table I we show the results of quantitative estimates of the surface peaks in different geometries. In the single alignment cases the calculations were carried out via numerical simulations⁴ with the use of a bulk vibration amplitude ($u_x = 0.078$ Å) and two-body thermal vibration

correlation coefficients.⁵ In the double alignment configuration, the values were estimated from a simple two-atom configuration for proton scattering and did not include the effects of the correlation. Also shown in Table I are the experimental results of Tromp *et al.* for 98-keV H⁺ scattering and of Culbertson, Feldman, and Silverman for 200-keV He⁺ scattering. Note that because of the Z_1/E scaling of the surface peak,⁴ these two scattering situations are essentially equivalent.

For [111] channeling all stacking models give a calculated surface peak that is close to the bulklike value. The small difference between models is due to a change in the atom spacing along the [111] strings. For [001] channeling there is an excess surface peak of 0.49, 1.17, and 1.50 atoms per row for the three models, respectively. This is equivalent to 0.98, 2.34, and 3.0 displaced monolayers since 1 atom per row corresponds to two monolayers for [001] channeling. The number of calculated excess monolayers is close to that expected from a simple inspection of Fig. 1. In the case of model . . . *BbC* [see Fig. 1(c)] the first displaced layer sha-

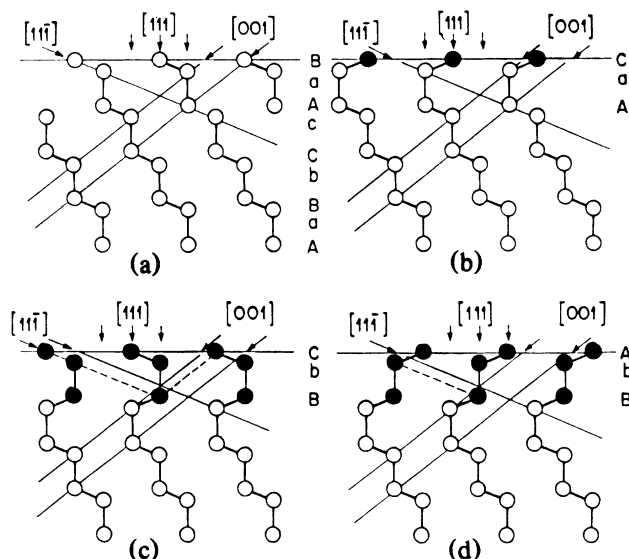


FIG. 1. Stacking sequence of atom layers for the bulk structure (upper left) and different faulted configurations in a side view of the (110) plane for a Si(111) surface. The models are denoted by their stacking sequence starting with the ninth layer into the bulk: (a) bulklike structure . . . *AaBbCcAaB*; (b) . . . *AaBbCcAa|C*; (c) . . . *AaBbCc|BbC*; (d) . . . *AaBbCc|Bb|A*. Also shown are the channeling directions for the incident beam. The dashed line in 1(c) denotes that the displaced atoms form a string which is aligned with the incident direction.

TABLE I. Surface peak (atoms/row) calculations for Si(111)-(1×1) including several types of stacking faults.

Direction ^a	Model				Expt.
	(Bulk) ... <i>AaB</i> [Fig. 1(a)]	... <i>Aa C</i> [Fig. 1(b)]	... <i> BbC</i> [Fig. 1(c)]	... <i> Bb A</i> [Fig. 1(d)]	
[111] _c	1.48	1.55	1.58	1.47	1.77 ± 0.09 ^b 1.7 ± 0.1 ^c
[001] _c	1.41	1.90	2.58	2.91	2.75 ± 0.14 ^b 2.6 ± 0.1 ^c
[11 $\bar{1}$] _c	1.52	2.42	2.90	3.71	3.7 ± 0.3 ^c
[111] _c + [111] _b	0.60		0.83	1.20	1.0 ± 0.05 ^c
[001] _c + [111] _b	0.90		1.81	1.87	1.8 ± 0.10 ^c

^aThe subscripts *c* and *b* indicate channeling and blocking directions, respectively.^bFrom Ref. 1.^cFrom Ref. 2.

dows the third displaced layer along a [001] direction; the scattering contribution from the third layer then depends on the beam parameters and vibrational amplitudes and requires the more complete calculation given here. For [11 $\bar{1}$] channeling 1 atom per row is equivalent to 1 monolayer and the excess surface peak corresponds to 1–3 monolayers of atoms for models in Figs. 1(b)–1(d).

The experimental values in Table I show that there is good agreement between the two bodies of data in the region of overlap. Not shown is the incident beam energy-dependence data of Culbertson *et al.* which is in very good agreement with the ...*|BbC* model [Fig. 1(c)]. Despite the quantitative agreement between the experimental results and the models, it is premature to make a definite assignment of the structure. The uncertainty in the model calculations primarily due to a lack of knowledge in the surface dynamics and the possible statistical errors in the experiment make a particular assignment difficult. Furthermore, the models are for (1×1) surfaces, while experimental results are for the (7×7) surface. A small fraction of displaced atoms at a model (7×7) surface would add a corresponding fraction to the surface peak, which would be close to the model uncertainties, ±0.2 layers. Nevertheless, it is seen from Table I that the basic concepts of a stacking-fault model can quantitatively explain the ion scattering data. It has been pointed out that a stacking-fault model predicts additional blocking minima which has not yet been observed.² This is probably due to the lack of perfect (1×1) symmetry with a single stacking-fault domain in Si(111)-(1×1) samples.

Additional evidence for a noncubic stacking of Si(111) surface layers comes from CMTA low-energy electron-diffraction (LEED) which displays mixed cubic-hexagonal symmetry rather than the trigonal symmetry expected for a bulklike structure. In Fig. 2 we show the experimental CMTA profiles for the (00), (10), and (01) beams. Such data are interpretable with single scattering theory including attenuation. The method has been successfully applied to Ni(111) and Ag(111), where the (fcc) stacking is clearly seen in the positions of CMTA profiles.⁶ Data were taken with a Faraday cup collector and four-circle goniometer⁷ over incidence angles 0°–30°. The (*hkl*) labels on each

panel of Fig. 2 indicate the calculated positions for the bulk reflections. The (10) and (01) beams correspond to [1 $\bar{1}$ 2] and [211] azimuths, respectively.

The (00) beam, having only perpendicular momentum

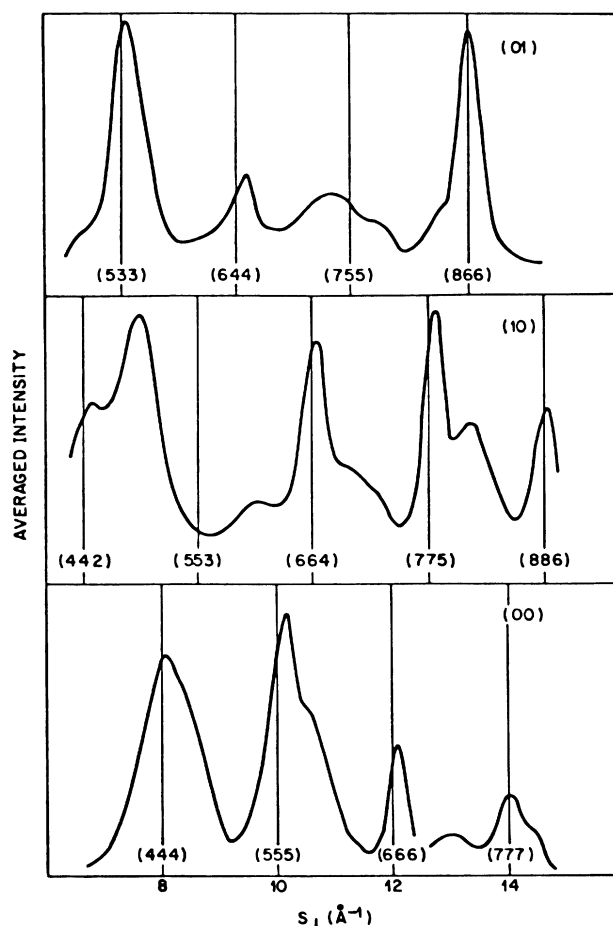


FIG. 2. Intensity profiles for low-energy electron diffraction on Si(111)-(7×7) averaged at constant momentum transfer S_{\perp} over incidence angles 0–30°. The bulk peak positions are indicated by vertical lines for the (00), (10), and (01) reciprocal-lattice rods.

transfer, is sensitive only to atomic displacements perpendicular to the surface. The intensity profile of this beam looks very bulklike,⁶ the peak maxima correspond to constructive interference between double layers, and their width indicates that only three to four double layers contribute appreciable intensity. Shoulders on the (444) and (555) peaks may indicate a small vertical relaxation such as a slight buckling, but the averaged profile is consistent with a nearly bulklike sequence of vertical distances. The bulk diamond structure factor differs from the fcc structure factor resulting in a modulation of peak intensities which extinguishes every fourth reflection; but this extinction rule appears not to hold for Si(111). For the nonspecular reflections (10) and (01), peaks are again present near their calculated positions, but, in addition, there are definite secondary peaks at the positions of the bulk reflections for the opposite beam. Stated simply, there is a mixed cubic-hexagonal symmetry of the (01) and (10) beam LEED pattern rather than the expected bulklike cubic threefold rotational symmetry. This mixing of (01) and (10) reflections is particularly apparent on the (10) beam for the peaks near $S_{\perp} = 7$ and 13 \AA^{-1} . The mixing is less apparent on the (01) beam yet still present, particularly near $S_{\perp} = 11 \text{ \AA}^{-1}$. Such secondary structure in the intensity profiles can result from a stacking fault in the surface layers, since the fault topology is equivalent to a 180° azimuthal rotation which changes the rotational symmetry from threefold towards sixfold. The apparent unequal mixing of the beams is due to a modulation of peak intensities arising from interference within the double layer. From the peak positions alone we cannot distinguish the (1×1) models under discussion. Although calculated kinematic profiles of a faulted structure of three layers [see Fig. 1(c)] gives too much intensity in the mixed reflections, there is no doubt that a faulted selvage model explains the symmetry of the CMTA data. The appearance of similar secondary structure in previous LEED measurements of the laser annealed (1×1) has been interpreted by full dynamical LEED theory in terms of vertical relaxation, $\sim 0.2 \text{ \AA}$, primarily in the first layer.⁸ This proposed structure is not in quantitative agreement with the ion scattering data, and the point here is that a faulted model can explain both LEED and ion scattering data.

The possibility that this new concept of noncubic stacking in the selvage could lead to models of (7×7) superlattices with two triangular domains has not gone unnoticed since this is consistent with previous work.⁹ The energy involved in faulting an otherwise undisturbed surface layer is undoubtedly small¹⁰ since the first- and second-neighbor coordination is unchanged.¹¹ Since the structures in Figs. 1(c) and 1(d) are equivalent within the limits of the model for ion channeling, we propose a new class of superlattice struc-

tures where the (7×7) unit cell is divided into two equal triangles with different stacking. This results in triangles with perimeters having near-neighbor top-layer atoms that could be π bonded or dimerized. The growth of this structure from the cleaved (2×1) surface could proceed by a triangular network of $\langle 112 \rangle$ -type shear displacements propagating from the linear (2×1) chains; this would also serve to relieve the residual strain of the cleaved surface. The detailed configuration of the (7×7) superlattice cannot be determined from the experimental results presented here; and hence a complete (7×7) picture is not appropriate here. Blocking effects reported by Tromp¹² from simulations of a (1×1) surface are also expected to be much weaker on a (7×7) surface with additional displaced atoms and three domain orientations.

Three recent experiments can be related to this type of stacking-fault model and resulting superlattice. Physisorption experiments with inert gas atoms on this surface find a single adsorption site in the (7×7) unit cell whose binding energy requires first-neighbor interactions with many more silicon atoms than provided by single vacancies, steps, or other models so far proposed.¹³ A vertex hole due to details of matching bonds provides such a site. The tunneling microscope experiment also finds a deep hole and 12 strong maxima in the unit cell.¹⁴ The interpretation of this corrugation pattern is currently under discussion; however, the triangular subunit structure is clearly displayed, and the hole might be due to edge and vertex matching conditions. Lastly, the deposition of thin layers of nickel on Si(111)- (7×7) results in near-perfect epitaxial growth of silicides that are rotated 180° with respect to that expected from a lattice-matched growth on a truncated bulk surface.¹⁵ A natural explanation for this is that the surface of the substrate, or part of it, is already rotated corresponding to the stacking faults discussed above.

In summary, we have shown that a new concept, a stacking-fault selvage region, is consistent with ion channeling and LEED rotational symmetry experiments. This concept, coupled with the previous idea of triangular domains, leads to a new surface structure which displays many of the properties observed in recent physisorption experiments, real-space studies with the tunneling microscope, and epitaxial silicide orientation results.

ACKNOWLEDGMENTS

It is a pleasure to thank D. R. Hamann, P. M. Petroff, L. C. Snyder, and M. J. Cardillo for helpful discussions, and we particularly thank M. B. Webb for suggesting the stacking-fault interpretation of the LEED data.

¹R. J. Culbertson, L. C. Feldman, and P. J. Silverman, *Phys. Rev. Lett.* **45**, 2043 (1980).

²R. M. Tromp, E. J. van Loenen, M. Iwami, and F. W. Saris, *Solid State Commun.* **44**, 971 (1982).

³L. F. Mattheiss and J. R. Patel, *Phys. Rev. B* **23**, 5384 (1981); H. Alexander, *J. Phys. (Paris) Colloq.* **40**, C6-27 (1979).

⁴I. Stensgaard, L. C. Feldman, and P. J. Silverman, *Surf. Sci.* **77**, 513 (1978).

⁵O. H. Nielsen and W. Weber, *J. Phys. C* **13**, 2449 (1980).

⁶T. C. Ngoc, M. G. Lagally, and M. B. Webb, *Surf. Sci.* **35**, 117 (1973).

⁷P. A. Bennett, Ph.D. thesis (Univ. of Wisconsin, Madison, 1980) (unpublished).

⁸D. M. Zehner, J. R. Noonan, H. L. Davis, and C. W. White, *J. Vac. Sci. Technol.* **18**, 852 (1981).

⁹E. G. McRae and C. W. Caldwell, *Phys. Rev. Lett.* **46**, 1632 (1981).

¹⁰M. T. Yin and M. L. Cohen, *Phys. Rev. B* **26**, 5668 (1982).

- ¹¹K. C. Pandey, Phys. Rev. Lett. 49, 223 (1982). In this reference it is, in fact, implicit that a hexagonal wurtzite overlayer is energetically less favorable than the π -bonded (2×11); J. E. Northrup and M. L. Cohen, Phys. Rev. Lett. 49, 1349 (1982).
- ¹²R. M. Tromp, Bull. Am. Phys. Soc. 28, 479 (1983).
- ¹³E. Conrad and M. B. Webb (private communication).
- ¹⁴G. Binnig, H. Rohrer, Ch. Gerber, and E. Weibel, Phys. Rev. Lett. 50, 120 (1983).
- ¹⁵R. T. Tung, J. M. Gibson, and J. M. Poate, Phys. Rev. Lett. 50, 429 (1983).